Cardiovascular Research 75 (2007) 498–509

Cardiovascular Research

www.elsevier.com/locate/cardiores

Dilated cardiomyopathy is associated with reduced expression of the cardiac sodium channel Scn5a

Michael Hesse[a], Colleen S. Kondo[b], Robert B. Clark[b], Lin Su[a], Frances L. Allen[a], Colleen T.M. Geary-Joo[a], Stanley Kunnathu[b], David L. Severson[c], Anders Nygren[d], Wayne R. Giles[b], James C. Cross[a,*]

[a] *Department of Comparative Biology and Experimental Medicine, Faculty of Veterinary Medicine, University of Calgary, Calgary, AB, Canada T2N 4N1*
[b] *Faculty of Kinesiology, University of Calgary, Calgary, AB, Canada T2N 4N1*
[c] *Department of Pharmacology and Therapeutics, University of Calgary, Calgary, AB, Canada T2N 4N1*
[d] *Centre for Bioengineering Research and Education, Electrical and Computer Engineering, University of Calgary, Calgary, Canada T2N 4N1*

Received 22 December 2006; received in revised form 16 March 2007; accepted 16 April 2007
Available online 21 April 2007
Time for primary review 27 days

Abstract

Objective: Dilated cardiomyopathy (DCM) leads to dilation of the cardiac chambers and congestive heart failure. Recent reports have associated mutations in the *SCN5A* gene, which codes for the major cardiac sodium channel Nav1.5, with DCM. Although DCM is the most common form of cardiomyopathy, no animal studies have established this functional connection.
Methods and results: We have produced transgenic mice that ectopically express the transcriptional repressor Snail in heart. These animals display severe DCM, ECG abnormalities, conduction defects, revealed by voltage-sensitive dye imaging, and significantly reduced voltage-gated sodium current as measured by patch clamping. There is a concomitant decrease in expression of the major cardiac sodium channel gene *Scn5a*, which we show by gene reporter assays and electrophoretic mobility shift assays is a direct target of Snail.
Conclusions: Our findings indicate that a decrease in *Scn5a* expression and significant reduction in sodium current can result in DCM, and support the hypothesis that some mutations in the human *SCN5A* gene can lead to DCM.

Keywords: Cardiomyopathy; Gene expression; Heart failure; Transgenic animal models; Na-channel

This article is referred to in the Editorial by Schulze-Bahr (pages 455–456) in this issue.

1. Introduction

Dilated cardiomyopathy (DCM) is the most common form of cardiomyopathy and is the leading indication for heart transplantations [1]. The underlying cause of DCM is an initial weakening of the myocardium followed by marked adaptive dilation as a consequence of the compromised pump function. More than 20 genes are associated with DCM in humans, including structural proteins of the sarcomere that transmit the contractile force and proteins associated with Ca^{2+} homeostasis [2]. Recently, mutations in ion channel genes have also been associated with DCM in humans. These include *ABCC9*, the gene encoding the subunit SUR2A of cardiac ATP-sensitive potassium channel [3] and *SCN5A*, which encodes the alpha subunit of the major Na^{+} channel in the heart, Nav1.5. Previously, *SCN5A* has been implicated in conduction disturbances and other electrophysiological phenotypes [4]. Gain-of-function mutations in *SCN5A* can cause a variant of the long QT syndrome

* Corresponding author. Department of Comparative Biology and Experimental Medicine, Faculty of Veterinary Medicine, University of Calgary, HSC Room 2279, 3330 Hospital Drive, N.W., Calgary, Alberta, Canada T2N 4N1. Tel.: +1 403 220 6876; fax: +1 403 270 0737.
E-mail address: jcross@ucalgary.ca (J.C. Cross).

0008-6363/$ - see front matter © 2007 European Society of Cardiology. Published by Elsevier B.V. All rights reserved.
doi:10.1016/j.cardiores.2007.04.009

due to abnormal myocardial repolarization. Loss-of-function *SCN5A* mutations are associated with Brugada syndrome. These patients have a high risk for developing arrhythmia and sudden death, although their hearts are reported to be structurally normal [5]. Some recent reports have also implicated *SCN5A* mutations in DCM [6,7] but the data are controversial because DCM may be secondary to long-lasting atrial arrhythmia [8] or tachycardia-induced cardiomyopathy [9].

The Snail family of zinc finger proteins are transcriptional repressors that regulate genes associated with cell–cell adhesion, epithelial to mesenchymal transition [10], and the transition to endoreduplication in trophoblast cells of the placenta, megakaryocytes and drosophila tissues [11]. Snail is expressed in the mouse embryonic heart during early intrauterine development [12]. In the present study, we discovered that transgenic mice expressing Snail in the postnatal heart show downregulation of the Scn5a Na^+ channel in the heart which in turn is associated with marked DCM in the absence of any arrhythmias.

2. Experimental procedures

2.1. Mice and genotyping

All experimental protocols were approved by the University of Calgary Animal Welfare Committee and followed the guidelines of the Canadian Council on Animal Care and conformed with the *Guide for the Care and Use of Laboratory Animals* published by the US National Institutes of Health (NIH Publication No. 85-23, revised 1996). The generation of MHC-Snail mice expressing the Snail cDNA under the control of the myosin heavy chain α promoter (TG [Myh6-Snai1]B10JCC) is described in Supplementary Material and Methods. They were genotyped by PCR using the primers 5′-CTTCCAGCCCTCTCTTTCTC-3′, 5′-CGTTTTCAGTTTCCGCAGTG-3′, amplifying endogenous Myh6 (450 bp) and 5′-CAGGTCGTGCAGACACAAGG-3′, representing Snail nucleotides 549–568, amplifying an 820 bp fragment of the Snail transgene with primer 5′-CTTCCAGCCCTCTCTTTCTC-3′. The PCR parameters were 30 s at 94 °C, 30 s at 61 °C and 60 s at 72 °C for 30 cycles. Hemi- and homozygous MHC-Snail mice were genotyped by Southern blotting with a 1.67 kb alpha-MHC probe to a 6 kb endogenous or 7.4 kb transgenic BamHI fragment of genomic DNA.

2.2. Histology and immunofluorescence staining

Hearts were dissected, washed in PBS and frozen in liquid nitrogen. Cryosections were fixed in acetone for 10 min at −20 °C. Sections were incubated with a 1:100 dilution of primary antibody against Cx43 (C-6219, Sigma) for 1 hour at RT, washed with PBS and incubated with secondary antibody anti-rabbit Cy3-conjugated (Chemicon International) for 30 min, washed in PBS and mounted. Fibrosis in cardiac sections was determined by Masson Trichrome stain (HT 15, Sigma).

2.3. Electron microscopy

Left ventricles were dissected from hearts, minced and fixed in 2% EM-grade glutaraldehyde (Sigma), 2% PFA in 0.2 M sodium cacodylate (pH 7.4; Sigma) overnight at 4°C, and post-fixed in 1% osmium tetroxide (EM Sciences) in 0.2 M sodium cacodylate (pH 7.4) for 2h at 4 °C. Tissue was dehydrated in increasing concentrations of ethanol up to 70%, treated in 2% uranyl acetate (ProSciTech) in 70% ethanol, and further dehydrated in increasing ethanol concentrations (70–100%). Tissue was treated with propylene oxide (EM Sciences) and resin embedded (EMBED 812 kit, EM Sciences).

2.4. Cell cultures and transfection

P19 mouse teratocarcinoma cells were cultured in αMEM plus 10% fetal bovine serum. Transient transfections were carried out using Lipofectamine (Invitrogen). Cells were plated at a density of 1×10^5 cells per well in 6 well dishes 24 h prior to addition of complexes containing 5 μl of lipofectamine and 4.2 μg of DNA (200 ng of pβActin-LacZ, 2 μg of P-+255, containing luciferase under control of a human Scn5a promoter segment from −261 to +255 [13], and the indicated amount of either pREP-mSna or pREP-mSnaΔSNAG expression vector [11]. Fresh medium was added 3h post-transfection, and cells were harvested after an additional 45 h. Luminescence levels were measured with a luminometer using a kit (Promega) and were normalized to β-galactosidase activity. Values are reported relative to empty pGL3 vector and represent means±SE for duplicate transfected dishes in 3 experiments.

2.5. Northern blot hybridization

RNA was extracted from whole hearts using Trizol (Invitrogen). RNAs were electrophoresed in MOPS/formaldehyde gels, capillary blotted, and UV-crosslinked onto nylon membranes (GeneScreen Plus, DuPont). Membranes were hybridized with random primed ^{32}P-labeled probes in hybridization buffer [14] at 60 °C overnight. A probe for mouse *Scn5a* was amplified by PCR and consisted of bp 2823 to 3253 of the *Scn5a* cDNA [15]. The probe for *GAPDH* has been described previously [15]. The membranes were washed in 20 mM sodium phosphate buffer (pH 7.2) containing 1% sodium dodecyl sulfate at 65 °C and exposed to X-ray film.

2.6. EMSA

Electrophoretic mobility shift assay was performed as described previously [11] using the oligonucleotides described in supplementary experimental procedures.

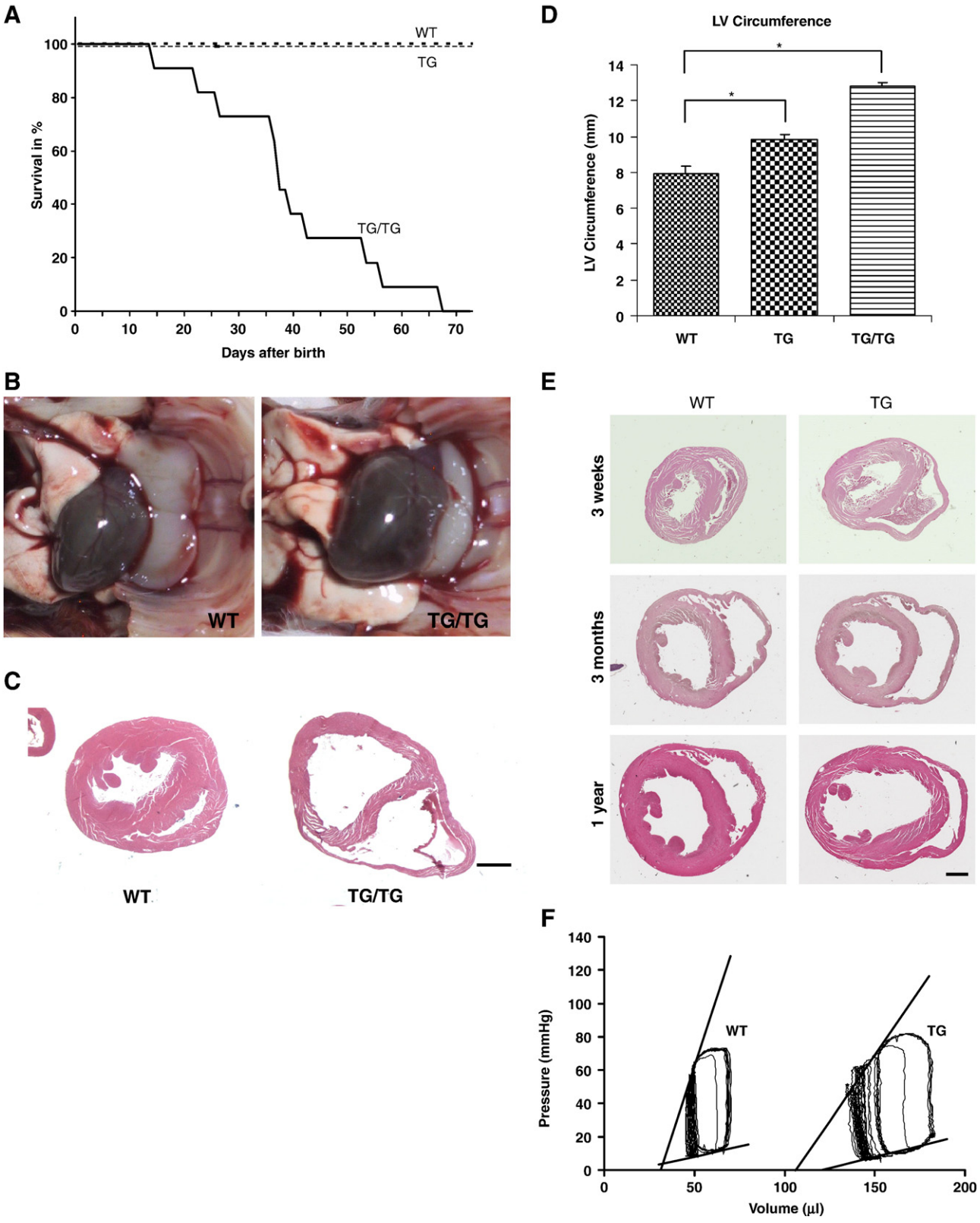

Fig. 1. TG/TG mice develop DCM and die within two months postnatally from cardiac failure while TG mice develop progressive DCM. (A) Survival curve for MHC-Snail mice with one (TG) or two (TG/TG) transgene copies compared to WT littermates ($n=11$ for all groups). (B) Hearts of TG/TG mice are significantly larger than hearts of WT mice. (C) HE staining of histological sections from WT and TG/TG hearts, demonstrating severe DCM in TG/TG hearts. (D) Left ventricular (LV) circumference is significantly increased in TG and TG/TG mice compared to WT mice at 3 weeks of age. Asterisks indicate $p<0.05$, $n=3$ for all groups. (E) HE staining of histological sections for WT and TG hearts at 3 weeks, 3 month, and 1 year of age, showing progressive DCM in TG mice. (F) Pressure-volume loops, obtained using the isolated working heart method, from WT and TG mice. The family of loops was aquired by temporarily stopping flow to the left atrium. Bars are 1 mm.

Table 1
Echocardiography of 3 and 5 weeks old WT, TG and TG/TG mice

	3 weeks			5 weeks		
	WT	TG	TG/TG	WT	TG	TG/TG
IVSd (mm)	0.62±0.03	0.65±0.06	0.59±0.08	0.67±0.04	0.79±0.07	0.66±0.08
IVSs (mm)	0.82±0.06	0.84±0.08	0.77±0.08	0.87±0.04	0.95±0.08	0.73±0.01
LVPWd (mm)	0.71±0.04	0.74±0.06	0.67±0.04	0.83±0.04	0.76±0.05	0.69±0.13
LVPWs (mm)	0.87±0.04	0.95±0.07	0.74±0.06	1.01±0.06	0.97±0.06	0.90±0.10
LVIDd (mm)	3.32±0.15	3.92±0.11 $p<0.05$	4.19±0.38 $p<0.05$	3.63±0.11	4.54±0.19 $p<0.05$	5.32±0.22 $p<0.05$
LVIDs (mm)	2.45±0.08	2.90±0.10 $p<0.05$	3.35±0.28 $p<0.05$	2.65±0.08	3.51±0.22 $p<0.05$	4.54±0.07 $p<0.05$
LVvold	48.06±3.41	74.16±5.91 $p<0.05$	87.26±16.49 $p<0.05$	59.31±4.34	101.92±8.96 $p<0.05$	148.69±13.65 $p<0.05$
LVvols	22.95±1.85	38.71±2.84 $p<0.05$	49.99±7.66 $p<0.05$	29.09±1.88	60.59±7.40 $p<0.05$	99.24±4.08 $p<0.05$
FS (%)	26.18±1.41	23.52±1.97	19.72±2.66 $p<0.05$	25.27±1.24	21.02±2.68	15.58±2.66 $p<0.05$

IVSd,s: Interventricular septum thickness measured at diastole or systole, respectively; LVPWd,s: Left ventricle posterior wall thickness at diastole or systole, respectively; LVIDd,s: Left ventricle internal diameter at diastole or systole, respectively; LVvold,s: Left ventricle volume at diastole or systole, respectively; FS: fractional shortening. $N=10$ for WT, $n=9$ for TG and $n=5$ for TG/TG.

2.7. RT-PCR

Reverse Transcriptase PCR was performed as previously described [16], using primers and conditions for *Scn5a*, *Scn1b*, and *Scn2b* as described in a previous paper [15].

2.8. Assessment of cardiac function by echocardiography

Echocardiograms (M-mode measurements) were obtained from conscious mice to assess systolic function, as previously described [17].

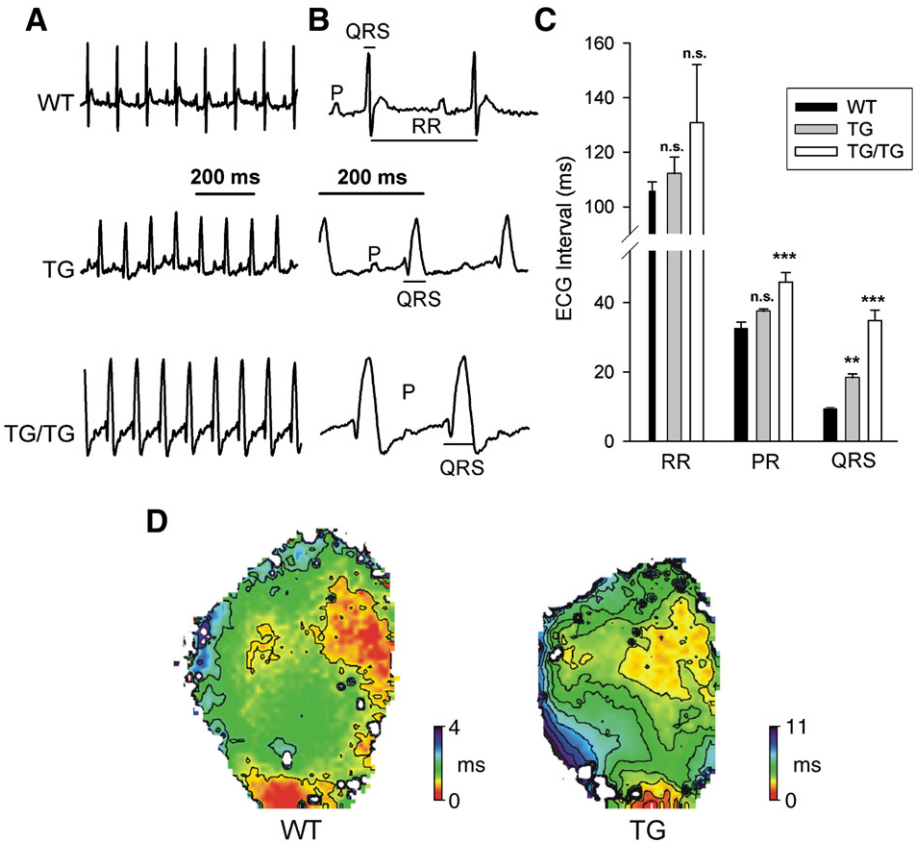

Fig. 2. TG mice exhibit slowed ventricular conduction. (A) Representative segments (0.75 s) of Lead I ECG recordings from WT, TG and TG/TG mice. (B) ECGs on an expanded time scale. 'P' wave, and 'RR' and 'QRS' intervals are indicated. 'PR' interval is from beginning of P wave to beginning of QRS complex. (C) Summarized ECG intervals from groups of 7 WT, 14 TG and 8 TG/TG mice. ** indicates $p<0.01$, and *** indicates $p<0.001$, compared with WT. (D) Activation maps acquired using voltage-sensitive dye mapping during spontaneous sinus rhythm for a WT and a TG heart. Points colored red represent areas on the ventricle first to depolarize, while points colored purple depolarize much later in the activation sequence. The isochrones (contours) shown are drawn at 1 ms intervals. Note that isochrones in the TG heart are spaced considerably closer together than in the WT heart, indicating significantly slower conduction of the waves of cardiac depolarization in the ventricles.

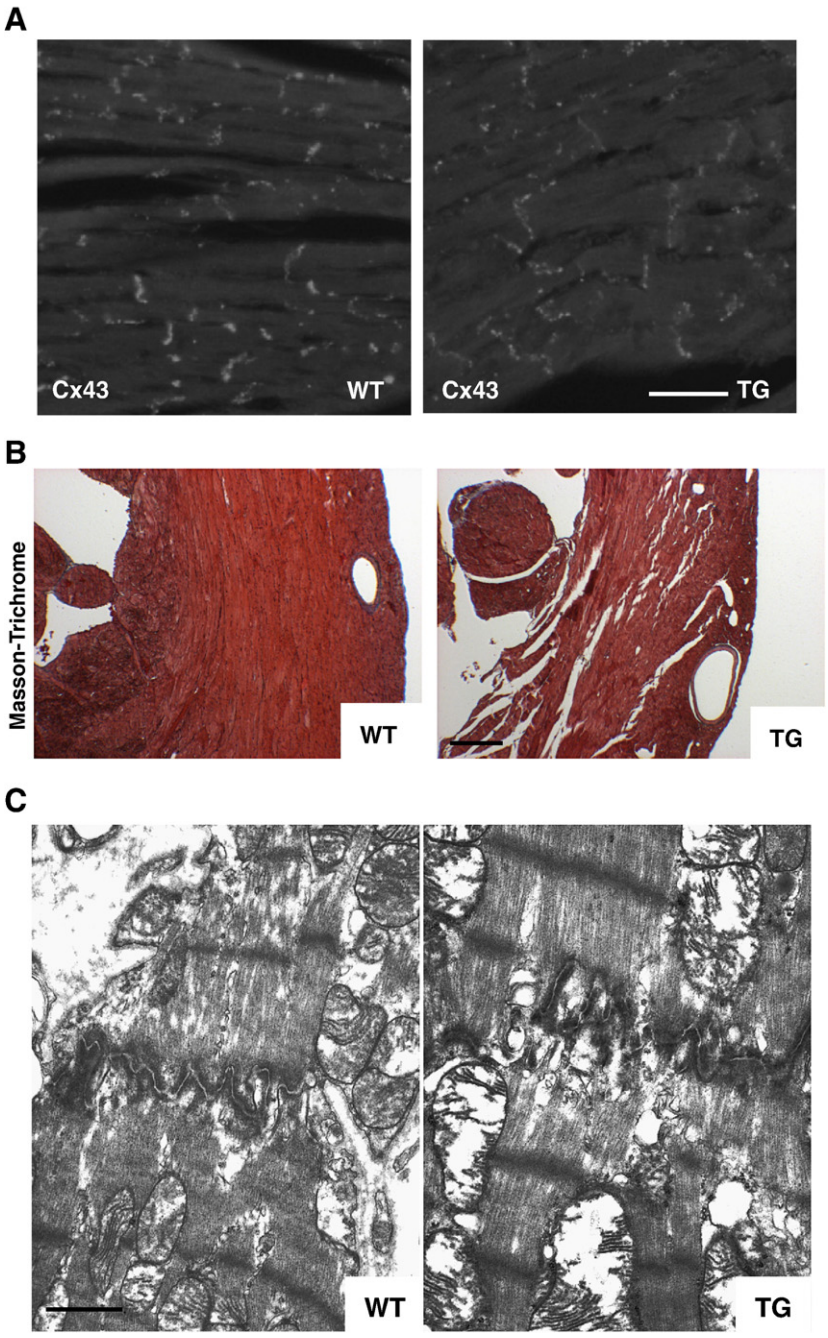

Fig. 3. Intercellular coupling of myocytes is not affected in TG mice. (A) Immunofluorescence staining for Cx43 expression in the ventricle myocardium of WT and TG mice. Cx43 stained the intercalated discs of cardiomyocytes and its distribution or intensity does not differ between WT and TG hearts. Bar is 50 μm. (B) Electronmicrographs of WT and TG cardiomyocytes revealed no differences in intercalated disc morphology or structure. Bar is 500 nm. (C) Mason-Trichrome staining of histological sections from WT and TG hearts showed no significant increase in fibrosis in TG hearts. Bar is 200 μm.

2.9. Electrocardiogram (ECG) measurements

ECGs were collected from constrained, conscious 3–4 week old WT, single gene copy (TG) and double gene copy (TG/TG) mice. Each animal was placed in a small apparatus (QRS Phenotyping Inc., Calgary, Canada) that was designed so that its feet made contact with gel electrode pads. This allowed collection of Lead I ECGs. Characteristic ECG waves and intervals were identified, measured, and tabulated using a semi-automated pattern recognition program (QRS Phenotyping Inc.).

2.10. Isolated, perfused working hearts

Mouse hearts were isolated, perfused and measured as described previously [18].

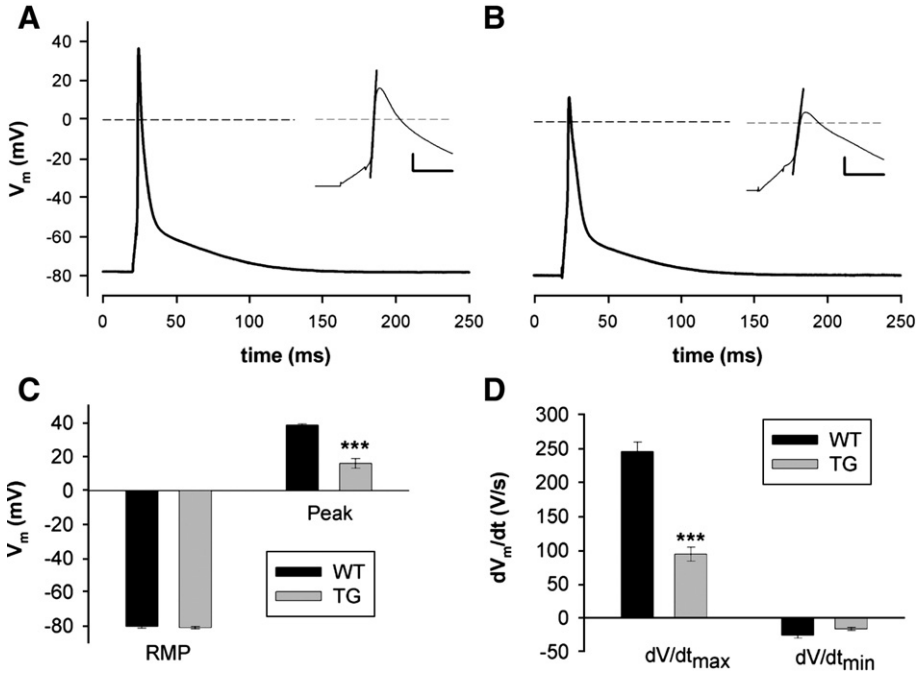

Fig. 4. TG ventricular myocyte action potential have decreased maximum upstroke rate and reduced overshoot. (A) Action potential from WT myocyte. Stimulation rate was 1 Hz. Inset shows the upstroke phase of the action potential on an expanded time scale. Vertical and horizontal bars indicate 20 mV and 3 ms, respectively. The solid straight line indicates dV/dt_{max}, which was 206 V/s. (B) Action potential from TG myocyte. dV/dt_{max} was 90 V/s. (C) Mean (±s.e.m.) resting membrane potential (RMP) and peak of action potential, from a group of 11 WT and 14 TG myocytes. (D) Mean dV/dt_{max} and dV/dt_{min} of action potentials from groups of WT and TG myocytes. *** indicates $p<0.0001$ compared with WT (Student's *t*-test). $p=0.0373$ for dV/dt_{min}.

2.10.1. Voltage-sensitive dye imaging

Voltage-sensitive dye imaging and data processing was performed as described previously [19,20].

2.11. Cardiomyocyte isolation and electrophysiology

Left ventricular myocytes were isolated from 3–4 week old WT and TG mice, using methods described previously [21]. Whole-cell patch clamp recordings of action potentials from isolated WT and TG myocytes were made as described elsewhere [21]. Voltage dependent Na^+ and K^+ currents were recorded as described in supplementary methods.

2.12. Statistics

Averaged values are expressed as mean±s.e.m. Statistically significant differences between mean values were determined with either Student's *t*-test or a one-way ANOVA test, as appropriate. A p value of <0.05 was considered to indicate significance.

3. Results

3.1. MHC-Snail transgenic mice suffer from severe DCM and die from cardiac failure

We have made transgenic mice that express the Snail transcription factor in the heart (Supplementary materials and methods). This expression is driven by the myosin heavy chain alpha gene promoter which turns on shortly after birth [22]. Hemizygous TG mice are viable, fertile, have a normal lifespan and display no obvious phenotype. However, when TG mice were intercrossed to obtain double-transgenic mice (TG/TG), all of them died by 2 months of age and 50% were dead within 36 days (Fig. 1A). Before death, TG/TG mice were smaller than their littermates, had laboured breathing and roughened fur, and were cyanotic. At necropsy, their hearts were enlarged with dilation of the ventricular chambers (Fig. 1B). Ascites was observed in several cases. Histological analysis of mice sacrificed at 3 weeks of age revealed dilation and thinning of the ventricular walls (Fig. 1C). Left ventricle wall thickness (LVWT), measured post mortem, was reduced in TG/TG mice (0.48±0.06 mm) compared to wildtype (WT) (1.00±0.02 mm) ($p=0.0013$), while the left ventricle circumference was significantly increased (Fig. 1D).

3.2. TG and TG/TG-mice develop a progressive DCM

The strong phenotype in TG/TG mice prompted us to more closely examine hemizygous TG mice. The left ventricle circumference was significantly increased at 3 weeks of age (Fig. 1D) and this dilation became more prominent at both 3 months and 1 year of age (Fig. 1E). Echocardiography showed that left ventricular diameter and volume was significantly greater in both TG and TG/TG mice at 3 and 5 weeks, while fractional shortening, as an indicator

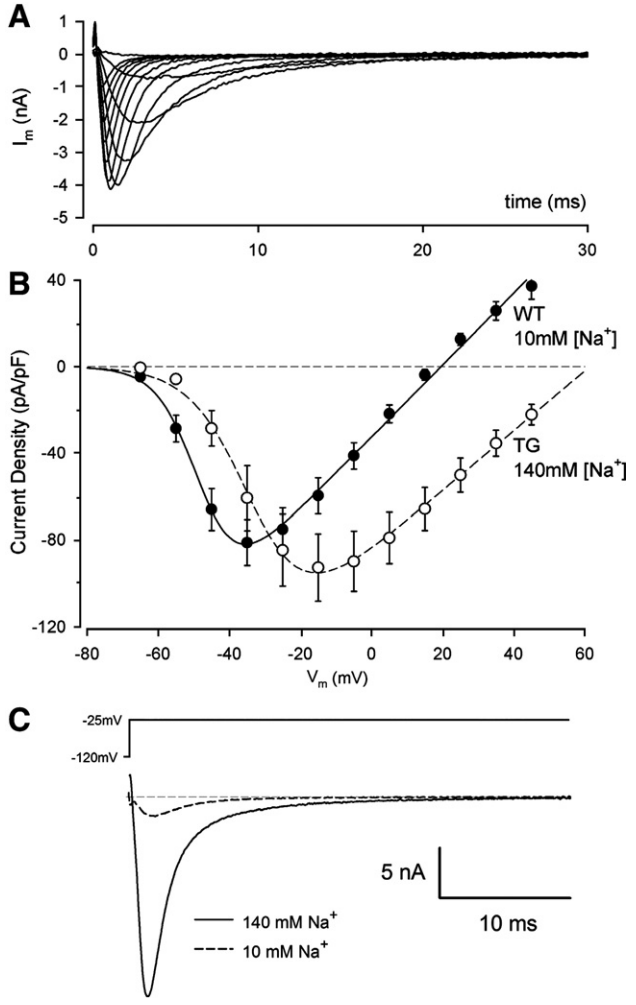

Fig. 5. The time- and voltage-dependent Na^+ current is significantly reduced in TG hearts. (A) Example of a family of Na^+ currents from a TG myocyte, in 140 mM $[Na^+]_o$ and 5 mM $[Na^+]_i$ at 15 °C. Cell was held at −120 mV, and stepped to between −65 mV and +45 mV, in 10 mV increments. Cell capacitance was 109.6 pF. (B) Current–voltage relations for WT and TG myocytes. $[Na^+]_o$ was 10 mM for WT and 140 mM for TG myocytes. $[Na^+]_i$ was 5 mM for both groups. $N=8$ for both groups. Continuous lines are best-fit Boltzmann functions. For WT: Vh=−47.8 mV, Sh=5.72 mV. For TG: Vh=−32.9 mV, Sh=8.15 mV. (C) Na^+ currents at −25 mV from a TG ventricular myocyte at 140 mM (solid line) and 10 mM (dashed line) $[Na^+]_o$. The decrease in current by a factor of about 10 in 10 mM $[Na+]_o$ was a necessary experimental manoeuvre to ensure reliable voltage clamp condition.

of cardiac performance, was unchanged in TG though was decreased in TG/TG mice (Table 1). The isolated working heart preparation was used to obtain a more detailed assessment of cardiac mechanics (Fig. 1F). Left ventricular volume increased almost two-fold in TG hearts compared to WT. Contractility, as determined by the slope of the end-systolic pressure-volume relation (ESPVR), was reduced by more than 50% (1.5188±0.968 ($n=5$) vs. 3.383±0.0681 ($n=6$), $p<0.05$). However, stroke volume (width of the loop) was unaffected. This was confirmed by the unchanged fractional shortening and normal lifespan in TG mice. The rightward volume shift and decreased ESPVR slope are typical characteristics of DCM. Taken together, the data strongly suggested that the ectopic expression of Snail in the heart lead to progressive DCM, even in hemizygous TG mice.

3.3. TG mice have slowed cardiac conduction

DCM can cause conduction delays and arrhythmias. Both types of abnormalities can be detected using electrocardiogram (ECG) analysis. In these studies there was relatively little difference in the heart rate (RR interval) amongst the three types of mice. However the QRS complex was longer in TG and TG/TG mice compared to WT (Fig. 2A–C). In addition, the PR interval, which is a measure of atrio-ventricular conduction time, was also longer in transgenic animals. Notably, no arrhythmias were detected during any of the recordings of TG or TG/TG mice. This is in accordance with the normal lifespan of TG mice and the fact that TG/TG mice die from progressive cardiac failure and not sudden death.

To assess ventricular activation and conduction in greater detail, the pattern and velocity of conduction in the left ventricle was measured. This was done using a voltage-sensitive dye in Langendorff perfused hearts of two month old TG mice. Conduction was slower in TG hearts compared to WT (activation isochrones are more closely spaced) (Fig. 2D). Specifically the 10–90% sinus rhythm activation time was more than doubled from 4.62 ms in WT ($n=6$) to 11.55 ms in TG hearts ($n=6$) ($p=0.02$). This increase in activation time is consistent with the broadening of the QRS complex in the ECG. Together, these data demonstrate that ventricular conduction in TG and TG/TG hearts was significantly slowed.

3.4. The intercellular coupling of myocytes is not affected in TG mice

The observed conduction abnormalities could have been caused by microanatomical changes in the conduction system, compromised intercellular coupling, or an intrinsic defect in ventricular myocytes. It is known that mis-expression of connexins can impair the cardiac conduction system, causing conduction abnormalities and arrhythmia [23]. Real-Time PCR for *Cx40*, *43*, and *45*, the three connexins expressed in the mouse heart, showed that their mRNA expression levels were not altered in TG mice (Supplementary Table 1). Staining with an antibody against Cx43 showed no changes in expression within intercalated discs or myocardium (Fig. 3A). Electron microscopy of myocytes from TG mice revealed no difference in intercalated disc structure (Fig. 3C). Conduction delays can also be caused by progressive fibrosis [23]. However, the amount and distribution of collagen detected by Masson-Trichrome staining in TG mice at 3 weeks (data not shown) or 1 year of age (Fig. 3B) was indistinguishable from WT.

3.5. Na^+ current is significantly reduced in TG hearts

In ruling out obvious changes in the cardiac conduction system or intercellular coupling, it was therefore likely that the

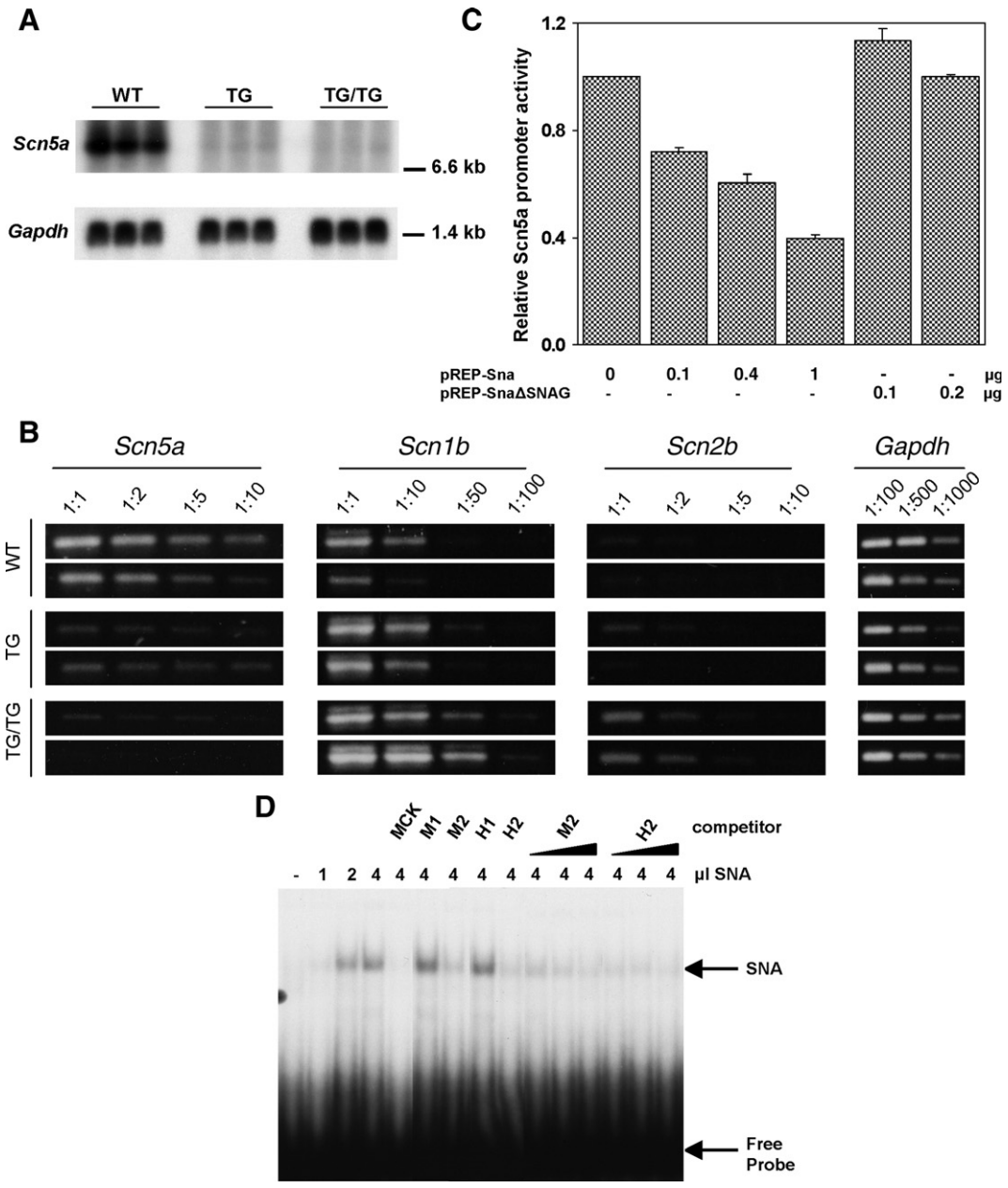

Fig. 6. Snail represses Scn5a expression in TG mice. (A) Northern Blot with a *Scn5a*-specific probe of WT, TG, and TG/TG hearts ($n=3$). A *Gapdh*-specific probe was used as a loading control. (B) RT-PCR with RNA from 2 weeks old WT, TG, and TG/TG mice ($n=2$). The cDNA was diluted as indicated and used for a PCR with Scn5a specific primers. PCR with *Gapdh*-specific primers was used to compare the cDNA starting amount. (C) Promoter reporter gene assay with luciferase driven by *Scn5a* promoter and transfection of different amounts of functional Snail expression vector (SNA) or an inactive Snail lacking the repressor domain (SNAG). (D) Electrophoretic mobility shift assay using a ^{32}P-labeled MCK E-box probe. The volume of *in vitro* translated mSNA used is indicated; lysate volume was equalized using control lysate. The position of the mSNA:E-box complex is indicated by an arrow. For competition assays, a 200-fold or increasing excess (50, 100, and 250 fold) of the indicated unlabeled sequence was used. NS, non-specific complex.

phenotype was caused by a cell-intrinsic defect. This was tested by patch-clamping of individual cardiomyocytes. While there was no difference in resting membrane potential, TG myocytes showed a reduced overshoot of action potentials (Fig. 4A–C). In addition, the maximum rate-of-rise (dV/dt_{max}) of action potentials was 2.6-fold lower in TG cells. The reduced upstroke rate of action potentials of TG myocytes, together with the broad QRS complex strongly suggested that the voltage-gated Na^+ current might be compromised. Voltage-clamp measurements of Na^+ currents were made in isolated WT and TG myocytes (Fig. 5A). In WT myocytes, external [Na^+] was reduced from 140 mM to 10 mM in order to reduce Na^+ currents to magnitudes at which adequate voltage-clamp conditions could be achieved (Fig. 5B). The TG cells could, however, be

adequately voltage-clamped in 140 mM external [Na^+] (Fig. 5A, B). Direct comparison of the Na^+ current at 10 mM to that at 140 mM external [Na^+] in a TG myocyte showed an approximately 10-fold reduction in magnitude of the Na^+ current (Fig. 5C).

3.6. Scn5a gene transcription is strongly repressed by the Snail transcription factor

The most likely explanation for the decrease in Na^+ current was a decrease of Nav1.5 expression since it is the major Na^+ channel. Indeed, microarray experiments showed that the gene that encodes it, *Scn5a*, was downregulated in TG mice (Supplementary Table 2). Northern blot and semi-quantitative RT-PCR analysis confirmed reduction in *Scn5a* mRNA in both TG and TG/TG mice compared to WT (Fig. 6A, B). The reduction in *Scn5a* mRNA was greater in TG/TG compared to TG mice and this correlated with the more severe phenotype. Expression of genes encoding the two β subunits that are known to bind to Nav1.5 [15] was increased in TG and TG/TG hearts (Fig. 6B), in accordance with microarray data (Supplementary Table 2). This increase was greater in TG/TG compared to TG mice and could be a compensatory mechanism.

The human and mouse *Scn5a* promoters contain several E-box motifs [13,24], which are binding sites for Snail [11]. To test this possibility directly, a luciferase reporter gene under the control of a human *Scn5a* promoter fragment and a Snail expression vector were co-transfected into P19 cells. Snail caused a dose-dependent reduction in *Scn5a* promoter activity, while transfection with an inactive Snail protein lacking the repressor domain (ΔSNAG), showed no effect (Fig. 6C). Oligonucleotides containing the sequences of two conserved E-box motifs were used in an electrophoretic mobility shift assay as competitors for binding to a known Snail binding motif from the muscle creatine kinase gene (MCK) [11]. Competitor oligonucleotides were generated for the mouse (M1, M2) and human (H1, H2) *Scn5a* promoter sequence, respectively. Snail was able to bind M2 and H2, but not M1 and H1 (Fig. 6D). These data indicate that Snail can directly bind to and repress the activity of the *Scn5a* promoter.

4. Discussion

We have shown here that ectopic expression of the Snail transcriptional repressor in the heart leads to DCM. Using a combination of approaches we have been able to associate the ventricular pathology with downregulation of the major Na^+ channel gene in the heart, *Scn5a*. While previous studies in humans have linked mutations in *SCN5A* with DCM, our results are the first to establish a functional connection between loss of Na^+ channel function and severe DCM. While there are several mouse models that develop DCM, this is the first model to be described in which DCM is the primary pathology as a consequence of reduced expression of a Na^+ channel α subunit.

4.1. MHC-Snail transgenic mice are a unique model of DCM

The Snail transgenic mouse model has several unique features that distinguish it from other animal models. First, while mutations in most DCM-associated genes in humans and mice result in other pathologies, such as muscular dystrophy, hypertrophic cardiomyopathy, lipodystrophy or restrictive cardiomyopathy, the mice described here displayed no additional phenotype. So far, only mutations in metavinculin and phospholamban show no overlap with other inherited diseases [2]. Second, TG/TG mice display a rapid onset of DCM as has been reported for MLP mutant mice [25]. In contrast TG mice show a slow progressive form, as in TIMP-3 knockout mice [26]. Interestingly, no arrhythmias were detected in either TG or TG/TG mice, whereas patients with loss-of-function mutations in SCN5A display a variety of conductance abnormalities. Fibrosis is a major cause of conduction disturbances and arrhythmia and in humans, myocyte loss by apoptosis, necrosis, or other mechanisms is common in DCM [27] and leads to interstitial fibrosis. The lack of fibrosis in the TG myocardium could explain the lack of arrhythmia and makes this TG mouse a good model for studying early events in DCM.

4.2. Is DCM due to Snail-mediated downregulation of Scn5a?

In searching for the mechanism underlying DCM in the MHC-Snail transgenic mice, we have concluded that it is most likely due to downregulation of the Scn5a Na^+ channel. This downregulation is mediated by Snail binding to and repressing the *Scn5a* promoter. The marked reduction in Na^+ current and related decrease in the dV/dt of the action potential lead to slower and hence less synchronous activation of the ventricular myocardium. This primary electrophysiological defect could, in turn, reduce contractility. In support of this model, we have observed the broadening of the QRS-complex, other ECG changes, and downregulation of *Scn5a* expression as early as 2 or 3 weeks of age and therefore well before dilation of the heart chambers has developed.

We have concluded that the effect of the transgene is due to ectopic expression of Snail *per se*, and not to the transgene insertion having a mutagenic effect based on two lines of evidence. First, the reduction in *Scn5a* gene expression and Na^+ channel activity is 80–90% even in single-TG mice and further reduced in TG/TG mice. These data are not consistent with a simple genetic model in which the transgene insertion compromises function of the adjacent genes. Second, in our initial efforts to develop the MHC-Snail transgenic mice, we had three founders, two of which died at a few months of age showing signs of heart failure (Supplementary materials and methods). Genotyping showed that one mouse had 10 and the other 4 copies of the transgene integrated into a single locus, whereas the surviving founder had only two.

Snail acts as a transcriptional repressor and more than 10 target genes have been identified, most of them components of adherens and tight junctions [10]. While we cannot completely rule out the possibility that cell–cell junctions are affected in the heart of MHC-Snail transgenic mice, there are no obvious morphological changes in individual cardiomyocytes that would indicate this. The cardiac adherens junction protein N-cadherin is not repressed by Snail, and *E*- and *VE-cadherin*, which are also targets of Snail, are not expressed in ventricular myocytes. Also, immunoflourescence staining for N-cadherin as well as β-catenin in TG hearts showed no differences compared to WT ventricular myocytes (data not shown). Members of the tight junction protein family are not expressed in the heart, which rules them out as possible Snail targets. Nevertheless there might be unknown targets of Snail, whose downregulation could cause DCM directly or indirectly. However, despite the fact that we do not have conclusive evidence, the data presented here is consistent with a direct downregulation of the expression of the major Na-channel Scn5a by Snail.

4.3. Human mutations in SCN5A and heart disease

Mutations in *SCN5A* that cause a decrease in Na^+ current are found in patients with Brugada syndrome and Lenègre disease. Brugada syndrome is characterized by an ST segment elevation in the right precordial ECG leads V1–V3, and a high incidence of sudden death caused by ventricular fibrillation [28]. Notably, patients with Brugada syndrome have structurally normal hearts. About 20% of all patients diagnosed with Brugada syndrome harbour mutations in *SCN5A* that cause a loss of channel function via different mechanisms [29]. Lenègre disease is associated with mutations in *SCN5A* in which the Na^+ current is decreased in cardiomyocytes leading to a conduction defect that is progressive and develops along with age-related myocardial fibrosis.

Recently reports have suggested a connection between mutations in *SCN5A* causing conduction disease and DCM [6,7]. In one study a D1275N mutation was identified in individuals with DCM [6]. Mutant channels were shown to activate at more positive voltages, which could result in reduced excitability of the myocytes [30]. However the authors could not determine whether DCM is a direct consequence of *SCN5A* mutation or is caused by chronic arrhythmia. In a second study with the same plus additional families, the D1275N mutation was confirmed and 4 different additional mutations in *SCN5A* were identified [7]. Of all individuals with a *SCN5A* mutation, 38% had overt DCM and 27% had early features of DCM. All of the mutations described in this report (D1275N, T220I, R814W, D1595H and 2550–2551 insTG) caused a reduction in Na^+-current. A recent paper based on a large Finnish family reported that the D1275N mutation is associated with cardiac conduction defects and atrial arrhythmia [31]. Dilation of ventricles was seen in only 4 out of 10 carriers. However, the mean age of the patients in this study was 27.6 years while the mean age at diagnosis of DCM in patients studied by McNair and by Olson was 47.9 years [7], implying a late onset of DCM. In another report it was shown that carriers of *Scn5a* mutations (R376H, R1023H, R1644C, I1968S) with structurally normal hearts and an average age of 44.8 years demonstrated cardiomyopathic changes such as myocardial cell degeneration and apoptosis [32]. This suggests a myocyte-intrinsic effect of certain *SCN5A* mutations that causes cardiomyocytes to lose their normal contractility and/or undergo cardiomyopathic changes, which in turn leads to dilation. In humans, it is very likely that this process takes several years and therefore does not necessarily manifest as DCM at the point of initial diagnosis of Brugada syndrome.

4.4. Functional links between Scn5a and DCM

In our mouse model, the Snail transgene is not expressed until birth, and therefore its effect is limited to late-developmental suppression of *Scn5a* expression. It therefore gives us a unique perspective on *Scn5a* function that is different from those gained from *Scn5a* knockout mice. *Scn5a* homozygous mutant mice have morphological abnormalities in the ventricular chamber and die around embryonic day 11.5 due to cardiac standstill [33]. Heterozygous mutant mice are viable and have a normal lifespan. However, cardiomyocytes from *Scn5a* heterozygous mutant mice have a 50% reduction of their cardiac Na^+ conductance, which causes impaired myocardial conduction *in vitro*. Aging Scn5a heterozygous mutants show progressive, age-related slowing of conduction, myocardial fibrosis, and changes in connexin expression [34,35], to some extent resembling Lenègre disease. These results from mutant mice as well as the data from patients carrying a loss-of-function mutation in *SCN5A* indicates that a 50% reduction during development has no effect on the gross morphology of the heart, but leads to conduction slowing and arrhythmia. It is possible that DCM is not observed in *Scn5a* heterozygous mutant mice, unlike some human patients with *SCN5A* mutations, simply because the lifespan of mice is not long enough for them to develop the pathology [33].

In our MHC-Snail transgenic model we have observed ~10-fold reduction in Na^+ current in juvenile and adult TG mice. The reduction is even more prominent in TG/TG mice. We were surprised that the MHC-Snail transgenic mice survive as long as they do, given the severity of the Na^+ channel defect and the fact that *Scn5a* null mutants are embryonic lethal. It may be that the late onset of the Snail expression delays the reduction in *Scn5a* until after the critical developmental period. Alternatively, the low level of *Scn5a* expression may just be enough to allow survival. Nonetheless, dramatic low-level expression of *Scn5a* leads to severe conduction defects and DCM in our mouse model. There is one report of compound heterozygosity for two different *SCN5A* mutations in humans that reduced the Na^+ current to 5–10% [36]. In this case report two affected individuals inherited the W156X nonsense-mutation from the father and the R225W missense mutation from the mother. One

individual died at 1 year of age due to intractable arrhythmia and an autopsy revealed severe DCM with myocardial fibrosis. The other individual displayed tachycardia after birth and broadening of the QRS-complex but recovered after β-blockade. However, conduction slowing progressed during the life of this individual.

Collectively, our data indicate that reductions in *SCN5A* function are associated with DCM. In addition though, it is clear that the level of the reduction of Na^+ current in cardiomyocytes is critical for the phenotypic outcome, varying between no changes, mild conduction delays, arrhythmia, or DCM. Also studies of these mice revealed a temporal connection between a reduction of Na^+ current and the time-course of the progressive DCM. The greater the reduction in Na^+ current, the faster the onset and progression of DCM, as seen in TG/TG mice, which develop a phenotype as early as 2 weeks of age and die within the first two months, while TG mice with a 90% reduction in Na^+ current have a normal lifespan. Extrapolated to humans, this would indicate that a reduction of 50% of Na^+ current, as seen in loss-of-function mutations in Brugada syndrome, would probably need several years to cause an obvious DCM. This is consistent with the late onset of DCM (average 47.5 years) in some patients with *Scn5a* loss-of-function mutations [6,7]. This means at least that DCM has to be taken into account as a possible long-term complication in patients with Brugada syndrome who are initially diagnosed with conduction defects. In addition, it is clear that Na^+ channel function and *SCN5A* expression should be considered as potential underlying mechanisms for DCM.

Acknowledgements

We thank O. Brusselers for technical assistance. We thank DM Roden for the Scn5a-promoter luciferase constructs. This work was supported by grants from the Canadian Institutes of Health Research (CIHR) (to J.C.C. and W.R.G.) and Heart and Stroke Foundation (W.R.G.). M.H. was supported by fellowships from the German Research Foundation (HE4477/1-1 and HE4477/1-2), and J.C.C. is an Investigator of the CIHR and a Scientist of the Alberta Heritage Foundation for Medical Research.

Appendix A. Supplementary data

Supplementary data associated with this article can be found, in the online version, at doi:10.1016/j.cardiores.2007.04.009.

References

[1] Maron BJ, Towbin JA, Thiene G, Antzelevitch C, Corrado D, Arnett D, et al. Contemporary definitions and classification of the cardiomyopathies: an American Heart Association Scientific Statement from the Council on Clinical Cardiology, Heart Failure and Transplantation Committee; Quality of Care and Outcomes Research and Functional Genomics and Translational Biology Interdisciplinary Working Groups; and Council on Epidemiology and Prevention. Circulation 2006;113:1807–16.

[2] Osterziel KJ, Perrot A. Dilated cardiomyopathy: more genes means more phenotypes. Eur Heart J 2005;26:751–4.

[3] Bienengraeber M, Olson TM, Selivanov VA, Kathmann EC, O'Cochlain F, Gao F, et al. ABCC9 mutations identified in human dilated cardiomyopathy disrupt catalytic KATP channel gating. Nat Genet 2004;36:382–7.

[4] George Jr AL. Inherited disorders of voltage-gated sodium channels. J Clin Invest 2005;115:1990–9.

[5] Brugada P, Brugada R, Antzelevitch C, Brugada J. The Brugada Syndrome. Arch Mal Coeur Vaiss 2005;98:115–22.

[6] McNair WP, Ku L, Taylor MR, Fain PR, Dao D, Wolfel E, et al. SCN5A mutation associated with dilated cardiomyopathy, conduction disorder, and arrhythmia. Circulation 2004;110:2163–7.

[7] Olson TM, Michels VV, Ballew JD, Reyna SP, Karst ML, Herron KJ, et al. Sodium channel mutations and susceptibility to heart failure and atrial fibrillation. JAMA 2005;293:447–54.

[8] Groenewegen WA, Wilde AA. Letter regarding article by McNair et al, "SCN5A mutation associated with dilated cardiomyopathy, conduction disorder, and arrhythmia". Circulation 2005;112:e9–e10.

[9] Adler E, Fuster V. SCN5A—a mechanistic link between inherited cardiomyopathies and a predisposition to arrhythmias? JAMA 2005;293:491–3.

[10] Barrallo-Gimeno A, Nieto MA. The Snail genes as inducers of cell movement and survival: implications in development and cancer. Development 2005;132:3151–61.

[11] Nakayama H, Scott IC, Cross JC. The transition to endoreduplication in trophoblast giant cells is regulated by the mSNA zinc finger transcription factor. Dev Biol 1998;199:150–63.

[12] Timmerman LA, Grego-Bessa J, Raya A, Bertran E, Perez-Pomares JM, Diez J, et al. Notch promotes epithelial-mesenchymal transition during cardiac development and oncogenic transformation. Genes Dev 2004;18:99–115.

[13] Yang P, Kupershmidt S, Roden DM. Cloning and initial characterization of the human cardiac sodium channel (SCN5A) promoter. Cardiovasc Res 2004;61:56–65.

[14] Church GM, Gilbert W. Genomic sequencing. Proc Natl Acad Sci U S A 1984;81:1991–5.

[15] Haufe V, Camacho JA, Dumaine R, Gunther B, Bollensdorff C, von Banchet GS, et al. Expression pattern of neuronal and skeletal muscle voltage-gated Na+ channels in the developing mouse heart. J Physiol 2005;564:683–96.

[16] Hemberger M, Hughes M, Cross JC. Trophoblast stem cells differentiate in vitro into invasive trophoblast giant cells. Dev Biol 2004;271:362–71.

[17] Semeniuk LM, Kryski AJ, Severson DL. Echocardiographic assessment of cardiac function in diabetic db/db and transgenic db/db-hGLUT4 mice. Am J Physiol Heart Circ Physiol 2002;283:H976–82.

[18] How OJ, Aasum E, Kunnathu S, Severson DL, Myhre ES, Larsen TS. Influence of substrate supply on cardiac efficiency, as measured by pressure-volume analysis in ex vivo mouse hearts. Am J Physiol Heart Circ Physiol 2005;288:H2979–85.

[19] Nygren A, Clark RB, Belke DD, Kondo C, Giles WR, Witkowski FX. Voltage-sensitive dye mapping of activation and conduction in adult mouse hearts. Ann Biomed Eng 2000;28:958–67.

[20] Nygren A, Kondo C, Clark RB, Giles WR. Voltage-sensitive dye mapping in Langendorff-perfused rat hearts. Am J Physiol Heart Circ Physiol 2003;284:H892–902.

[21] Brouillette J, Clark RB, Giles WR, Fiset C. Functional properties of K+ currents in adult mouse ventricular myocytes. J Physiol 2004;559:777–98.

[22] Gulick J, Subramaniam A, Neumann J, Robbins J. Isolation and characterization of the mouse cardiac myosin heavy chain genes. J Biol Chem 1991;266:9180–5.

[23] Priori SG, Napolitano C. Genetics of cardiac arrhythmias and sudden cardiac death. Ann N Y Acad Sci 2004;1015:96–110.

[24] Shang LL, Dudley Jr SC. Tandem promoters and developmentally regulated 5′- and 3′-mRNA untranslated regions of the mouse Scn5a cardiac sodium channel. J Biol Chem 2005;280:933–40.

[25] Arber S, Hunter JJ, Ross J, Hongo M, Sansig G, Borg J, et al. MLP-deficient mice exhibit a disruption of cardiac cytoarchitectural organization, dilated cardiomyopathy, and heart failure. Cell 1997;88:393–403.
[26] Fedak PW, Smookler DS, Kassiri Z, Ohno N, Leco KJ, Verma S, et al. TIMP-3 deficiency leads to dilated cardiomyopathy. Circulation 2004;110: 2401–9.
[27] Kostin S, Pool L, Elsasser A, Hein S, Drexler HC, Arnon E, et al. Myocytes die by multiple mechanisms in failing human hearts. Circ Res 2003;92:715–24.
[28] Brugada P, Brugada J. Right bundle branch block, persistent ST segment elevation and sudden cardiac death: a distinct clinical and electrocardiographic syndrome. A multicenter report. J Am Coll Cardiol 1992;20: 1391–6.
[29] Priori SG, Napolitano C, Gasparini M, Pappone C, Della BP, Giordano U, et al. Natural history of Brugada syndrome: insights for risk stratification and management. Circulation 2002;105: 1342–7.
[30] Groenewegen WA, Firouzi M, Bezzina CR, Vliex S, van L. I, Sandkuijl L, et al. A cardiac sodium channel mutation cosegregates with a rare connexin40 genotype in familial atrial standstill. Circ Res 2003;92:14–22.
[31] Laitinen-Forsblom PJ, Makynen P, Makynen H, Yli-Mayry S, Virtanen V, Kontula K, et al. SCN5A mutation associated with cardiac conduction defect and atrial arrhythmias. J Cardiovasc Electrophysiol 2006;17:480–5.
[32] Frustaci A, Priori SG, Pieroni M, Chimenti C, Napolitano C, Rivolta I, et al. Cardiac histological substrate in patients with clinical phenotype of Brugada syndrome. Circulation 2005;112:3680–7.
[33] Papadatos GA, Wallerstein PM, Head CE, Ratcliff R, Brady PA, Benndorf K, et al. Slowed conduction and ventricular tachycardia after targeted disruption of the cardiac sodium channel gene Scn5a. Proc Natl Acad Sci U S A 2002;99:6210–5.
[34] Royer A, van Veen TA, Le BS, Marionneau C, Griol-Charhbili V, Leoni AL, et al. Mouse model of SCN5A-linked hereditary Lenegre's disease: age-related conduction slowing and myocardial fibrosis. Circulation 2005;111:1738–46.
[35] van Veen TA, Stein M, Royer A, Le QK, Charpentier F, Colledge WH, et al. Impaired impulse propagation in Scn5a-knockout mice: combined contribution of excitability, connexin expression, and tissue architecture in relation to aging. Circulation 2005;112:1927–35.
[36] Bezzina CR, Rook MB, Groenewegen WA, Herfst LJ, van der Wal AC, Lam J, et al. Compound heterozygosity for mutations (W156X and R225W) in SCN5A associated with severe cardiac conduction disturbances and degenerative changes in the conduction system. Circ Res 2003;92: 159–68.